Tadpole-shaped Au nano-particles fabricated by laser fragmentation of Au nano-spheres in liquid

Chong Zhang (张 冲), Jiaqi Ma (马佳琪), Dongdong Zhu (朱东东), Liang Liu (刘 良), Dameng Wang (王大猛), Xiangdong Liu (刘向东), and Ming Chen (陈 明)*

School of Physics, Shandong University, Jinan 250100, China
**Corresponding author: chenming@sdu.edu.cn*

Received January 4, 2016; accepted June 14, 2016; posted online July 25, 2016

Tadpole-shaped Au nano-particles with controllable tails are successfully fabricated by simply using laser fragmentation of separated Au nano-spheres in liquid. The optimum laser power densities (1.5–3 GW/cm^2) can enable part of the individual Au nano-sphere to be re-melted, released, and ultra-rapidly recondensed/crystallized on the outside of the original region. We find that the length of the tail in a tadpole-shaped Au nano-particle significantly increases from about 10 to 25 nm by increasing the laser power density. Benefiting from the unique structural features, the localized surface plasmon resonance (LSPR) absorption spectra of the tadpole-shaped Au nano-particles become broader by increasing the tail length. Moreover, the LSPR absorption band also exhibits a noticeable red shift from about 520 to 650 nm. Our results provide a convenient and valuable strategy to fabricated novel anisotropic-shaped nano-structures with fascinating properties.

OCIS codes: 140.3390, 220.4241, 300.1030.
doi: 10.3788/COL201614.081403.

Gold nano-materials (Au NMs) with controlled sizes and shapes have received increasing attention for decades because of their unique and tunable morphology-dependent physicochemical features. The peculiar properties associated with remarkable electron transport will render them highly desirable in extensive applications, such as superactive photo-catalysts, fast-response biosensors, photodynamic therapy, and ultrasensitive fluorescent probes[1–6]. Most importantly, the enhanced localized surface plasmon resonance (LSPR) of Au NMs in visible or near-infrared frequencies has provided the possibilities of using them for photovoltaic performance/optical applications, in vivo anatomical imaging, and early stage tumor diagnosis with deep tissue penetration[1,7–9]. To succeed in the manipulation of LSPRs in the visible and near-infrared regions, much interest has been aroused in the fabrication of anisotropic-shaped Au NMs owing to their unique multipolar plasmon resonance modes. It has been recognized that the multipolar plasmon resonance modes supported by anisotropic-shaped Au NMs should be precisely correlated with the desired crystal orientation, crystal structure, and NM sizes and shapes[4,6]. Consequently, tremendous efforts have been especially devoted to the controlled synthesis of anisotropic-shaped Au NMs, such as nano-rods, nano-prisms, nano-cages, nano-bipyramids, nano-rices, and nano-wires. In addition to these Au NMs, other novel and complex anisotropic nano-structures should also be designed, as they will be extremely valuable in nano-science and significant applications. Meanwhile, the related specific applications by using anisotropic-shaped Au NMs are often complicated because of the potential toxicity issues arising from the inevitable purification procedures via standard chemical fabrication based on the reduction of a precursor salt with a reducing agent. The development of new methods of conveniently synthesizing novel anisotropic-shaped Au NMs is important.

Recently, laser fragmentation in an activated solution has become an attractive green strategy to the fabrication of novel meta-stable phases of materials owing to the non-equilibrium processing character[3,10–18]. The scheme, which is environmentally friendly and has negligible toxicity, offers a breakthrough in toxicity challenges. Over the past decade, many interesting works, such as the controlled synthesis of ZnO-Zn composite nano-particles[15], the reconstruction of α-Ag_2WO_4 nano-rods[18], and the fabrication of hollow MgO nano-particles[17], have been devised using laser ablation in liquid. Recently, we reported the successful synthesis of ZnO porous nano-cages[13], zinc hydroxyl dodecylsulfate (ZHDS) nano-sheets[12], and TiO_2 nano-cages[11] by laser irradiation in an activated solution. Hence, it is very necessary to explore novel anisotropic-shaped Au NMs by the laser fabrication technology.

Herein, for the first time, we design a simple, versatile, and rapid route to controllably synthesize tadpole-shaped Au nano-particles with tunable tails based on laser fragmentation of mono-dispersed Au nano-spheres in liquid. The laser power density (1.5–3 GW/cm^2) plays a critical role in the fabrication of the novel anisotropic-shaped Au nano-particles. It can enable part of the individual Au nano-spheres to be released and ultra-rapidly recondensed/crystallized on the original region. In addition, the length of the tail in tadpole-shaped Au nano-particles can be increased from about 10 to 25 nm, with the laser power ranging from 1.5 to 3 GW/cm^2. The LSPR absorbance spectrums of the unique anisotropic-shaped Au NMs broaden and are significantly red shifted from about 520 to 650 nm. Meanwhile, a detailed discussion of the relevant mechanism is addressed. The aim of this work is to extend

to a new method of synthesizing the novel anisotropic-shaped Au NMs. In the future, it will be very beneficial to the fabrication of other complex nano-structures.

In a typical experiment, the mono-dispersed Au NMs should be firstly fabricated by the laser ablation of an Au plate in liquid. A well-polished, pure (99.99%) gold target was placed on the bottom of a rotating glass dish at a speed of ~150 rpm and that was filled with 0.5 mol/L cetyltrimethyl ammonium bromide (CTAB) and 10 mL distilled water. The CTAB is a dispersing and stabilizing agent in this experiment. A *Q*-switched Nd-YAG laser (Quanta Ray, Spectra Physics) beam operating at a wavelength of 1064 nm with a pulse duration of 10 ns and a 10 Hz repetition rate was focused on the Au target surface. A laser beam with a power density of 9 GW/cm^2 was focused on the Au surface by a quartz lens with 45 mm focal length. The laser ablation lasted for 50 min, and then the products were centrifuged at 10000 rpm for 15 min by an ultracentrifuge. The sediments were carefully transferred to a quartz tube and mixed with 5 mL distilled water. Finally, the as-prepared Au colloid solutions were irradiated by an unfocused laser beam with optimum laser power densities (1.5–3 GW/cm^2) for 40 min. The laser power density was monitored by an energy meter (Molectron, EPM 1000). After laser fabrication, the obtained Au NMs were repeated centrifuged at 10000 rpm for 10 min and carefully washed in distilled water two times. The sediments were dropped on a copper mesh and dried in an oven for observation by transmission electron microscopy (TEM; JEOL-JEM-2100 F). The LSPR absorbance spectrums of the Au NMs were measured with a UV-Vis-IR spectrometer (UV-1800, Shimadzu).

After a cumulative pulse laser ablation of pure Au metal in distilled water using 0.5 mol/L CTAB as the dispersing and stabilizing agent, low-magnification and high-resolution images of the Au NMs were analyzed by TEM [Figs. 1(a) and 1(b), respectively]. The typical TEM image in Fig. 1(a) clearly shows that numerous liquid-dispersed and well-defined spherical-like nano-particles with size dispersion 7%–10% are likely to be fabricated one by one individually and are not hinge jointed. The inset in Fig. 1(a) illustrates that the morphology of the representative nano-spheres is characterized by a highly center-symmetrical structure. The average diameter of these as-prepared nano-spheres is about 65 nm by measuring the size of the more than 200 particles in sight on the TEM images with the aid of the graphics editing program of Macromedia Fireworks 8. The high-resolution TEM (HRTEM) image in Fig. 1(b) provides a typical structural detail of the nano-sphere. The Au nano-sphere is found to be crystalline, according to the clear lattice fringes. The typical region with a periodicity corresponding to a d-spacing of 0.235 nm could be indexed with reference to the Au (111) plane structure. After unfocused laser irradiation of the as-prepared Au nano-spheres with a power density of 1.5 GW/cm^2, the typical low- and higher-resolution morphologies of the generated Au nano-particles were collected in Figs. 1(c) and 1(d). As shown in Fig. 1(c),

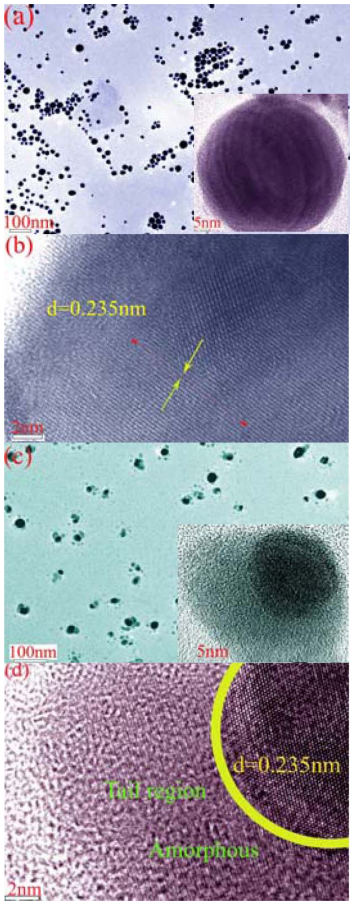

Fig. 1. (a) Typical low magnification of the nano-particles by the laser ablation of the pure Au metal in the solution. The inset shows the enlarged TEM image of the individual Au nano-spheres. (b) The HRTEM image of the Au nano-spheres. (c) The representative low-magnification TEM image of the Au nano-particles fabricated by unfocused laser beam irradiation of Au nano-spheres with a power density of 1.5 GW/cm^2. The inset in panel (c) shows the typical tadpole-shaped Au NMs. (d) The HRTEM image of the tadpole-shaped Au NMs.

compared with the center-symmetrical Au nano-spheres, the liquid-dispersed nano-particles indeed have different morphologies, which should be regarded as novel anisotropic-shaped Au NMs. A closer view of the representative nano-particles in the inset indicates that the product is a core structure, and the regions are covered and accreted with tail-like structures. The average length of the tail is about 10 nm by measuring the tails of more than 200 particles. After laser irradiation, the average diameter of the gold nano-core is about 24 nm. It is distinctly from that of the core-shell nano-particles, where the core is completely and entirely coved with the shell. The novel anisotropic-shaped Au NMs with the obvious core-tail structure will be named tadpole-shaped Au NMs in this Letter. The HRTEM image in Fig. 1(d) offers a typical structural detail of the cross region between the core and tail. The core region with a d-spacing of 0.235 nm is indexed as the (111) plane in the Au structure, implying that the core of the Au nano-spheres will be unaffected during laser fabrication. In

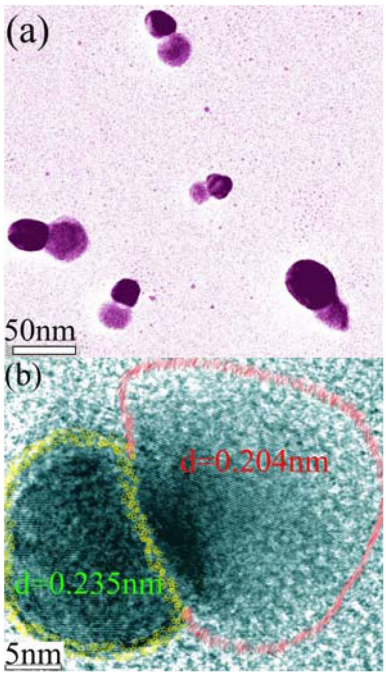

Fig. 2. (a) Representative low-magnification and (b) enlarged TEM images of the tadpole-shaped Au NMs by laser irradiation of Au nano-spheres with a power density of 3 GW/cm^2, respectively.

addition to the crystalline structure of the core, it is further noted that the tail of the tadpole-shaped Au NMs should be an amorphous material without any lattice fringes. We increased the laser power density to 3 GW/cm^2 and found that the tadpole-shaped Au NMs with even more obvious tails were obtained, as illustrated in Fig. 2(a). The mean length of the tail in the Au NMs is about 25 nm, which is significantly longer than that in Fig. 1(c). Moreover, the tail is also found to be crystalline according the clear lattice fringes in the HRTEM image [Fig. 2(b)]. Correspondingly, the lattice fringes with a spacing of 0.204 nm can be identified for the Au (200) plane. The tadpole-shaped Au NMs with crystalline structures can be fabricated by relatively higher laser irradiation. It is reasonable to deduce that the laser fabrication with the optimum laser power density can enable part of the individual Au nano-spheres to be released and recondensed/crystallized on the original region, resulting in the formation of the tail-core structure.

The possible growth of the novel anisotropic-shaped Au NMs is also different from the laser-induced layer-by-layer surface vaporization that causes the size reduction and mono-dispersion of the nano-particles[3]. In the following, we will describe the formation mechanism of the tadpole-shaped Au NMs. Before we reveal the mechanism, it is worth noting that lower or too-high laser power densities (less than 1.5 GW/cm^2 and higher than 3 GW/cm^2) cannot result in the obvious tadpole-shaped structure. The insufficient laser densities will fail to remove the Au material from the nano-sphere. Conversely, the separated Au nano-spheres will be completely divided

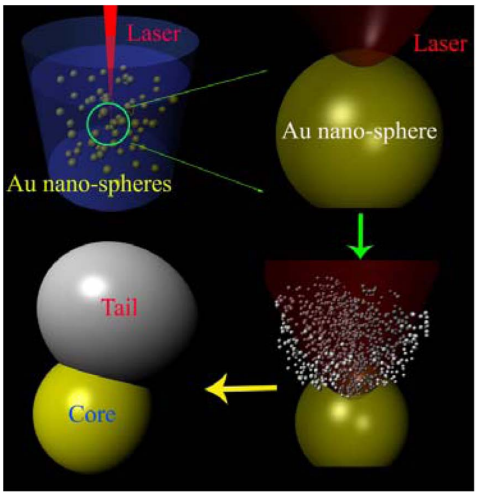

Fig. 3. Schematic growth of the tadpole-shaped Au NMs via the laser fragmentation of the individual Au nano-sphere in liquid.

into much smaller nano-particles by adopting too-high laser densities. A moderate laser power ranging from 1.5–3 GW/cm^2 is the optimum condition for the formation of tadpole-shaped Au NMs. Figure 3 provides a schematic diagram of the formation of anisotropic-shaped Au NMs. Due to the sufficient photon density, linear and non-linear optical absorption processes occur at the contact surface when the laser beam hits an individual Au nano-sphere. In this case, localized thermal processes like thermionic emission, vaporization, boiling, and melting should lead to an instantaneous Au material detachment process. Then, the released Au material will continue to be ultra-rapidly recondensed/crystallized on the outside of the original region. The formation of tadpole-shaped structures is related to the laser-induced localized detachment of the matter from individual Au nano-spheres and then recondensation/crystallization of the released matter on the original surface.

Following this mechanism, a higher laser power density should improve the degree of the localized vaporization and then increase the length of the tail in tadpole-shaped Au NMs. The mean length of the tail as a function of the laser power density is displayed in Fig. 4(a). The mean length increases from about 10 to 25 nm as the laser power density increases from 1.5 to 3 GW/cm^2, and the detailed length evolution can be described as a power-exponential function. Meanwhile, the average diameter of the Au spheres (core) decreases non-linearly from about 23 nm to 12 nm with an increase of the laser power density, as shown in Fig. 4(a). Moreover, the inset in Fig. 4(a) shows that the increasing the laser power density leads to a significant change in the solution color from light red to purple-gray. Finally, the unique LSPR absorbance features of the novel anisotropic-shaped Au NMs are illustrated in Fig. 4(b). Compared with the result of the Au nano-spheres, it is interesting to note that the LSPR absorbance spectrum becomes much broader. As shown in Fig. 4(b), the full width at half-maximum of the spectral

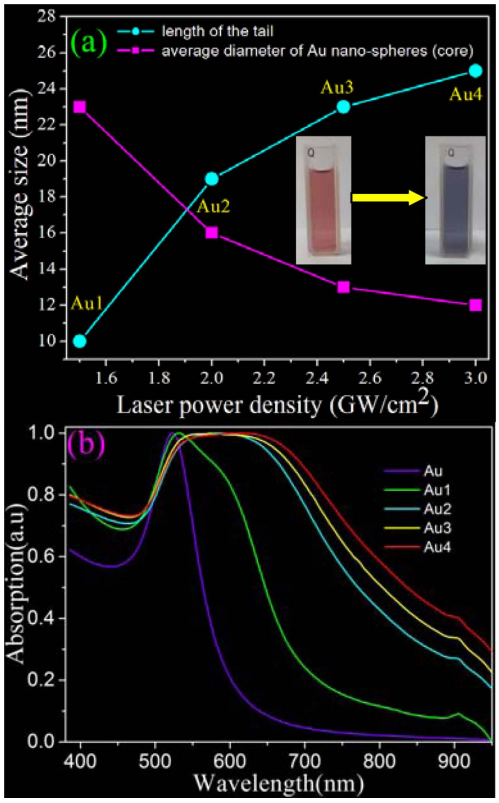

Fig. 4. (a) Curve of the mean length of the tail in tadpole-shaped Au NMs versus the laser power density. (b) The LSPR absorbance spectrums of the Au nano-spheres and tadpole-shaped Au NMs.

line increases from about 170 to 450 nm by increasing the tail length. The broadened LSPR absorption can be attributed to the mixed latitudinal and longitudinal plasmon wavelengths of the tadpole-shaped Au NMs. Moreover, the LSPR absorbance peak drastically red shifted from about 520 nm for Au nano-spheres to about 650 nm for the tadpole-shaped structures. The new construction of tadpole-shaped Au NMs with broadened absorption in visible region has significant implications for biological imaging and biomedicine.

In conclusion, we successfully demonstrate a facile and attractive strategy to controllably synthesize novel anisotropic-shaped Au NMs with tadpole-like structure by the laser fabrication of separated Au nano-spheres in liquid. The related mechanisms should be highly related to the fact that the laser beam induces the localized detachment of the matter from the individual Au nano-sphere. The released material will be recondensed/crystallized on the original surface, leading to the generation of tadpole-shaped Au NMs. In addition to the broadened LSPR absorbance spectral lines, the absorbance peaks of the tadpole-shaped Au NMs present a significantly red shift from about 520 to 650 nm with the increase of the laser power density. The laser-induced tadpole-shaped Au NMs with excellent LSPR spectra in the visible region will open up exciting classes of novel anisotropic-shaped noble nano-particles for photodynamic therapy applications in the future.

This work was supported by the National Natural Science Foundation of China (Nos. 11575102, 11105085, and 11375108) and the Fundamental Research Funds of Shandong University, China (No. 2015JC007).

References

1. M. S. Yavuz, Y. Y. Cheng, J. Y. Chen, C. M. Cobley, Q. Zhang, M. Rycenga, J. W. Xie, C. Kim, K. H. Song, A. G. Schwartz, L. V. Wang, and Y. N. Xia, Nat. Mater. **8**, 935 (2009).
2. X. Zhuo, X. Zhu, Q. Li, Z. Yang, and J. Wang, ACS Nano. **9**, 7523 (2015).
3. R. C. Luo, C. Li, X. W. Du, and J. Yang, Angew. Chem. Int. Ed. **54**, 4787 (2015).
4. J. P. Juste, L. M. Liz-Marzan, S. Carnie, D. Y. C. Chan, and P. Mulvaney, Adv. Funct. Mater. **14**, 571 (2004).
5. M. Cargnello, R. Agarwal, D. R. Klein, B. T. Diroll, R. Agarwal, and C. B. Murray, Chem. Mater. **27**, 5833 (2015).
6. H. S. Li, H. B. Xia, D. Y. Wang, and X. T. Tao, Langmuir **29**, 5074 (2013).
7. S. E. Skrabalak, J. Y. Chen, Y. G. Sun, X. M. Lu, L. Au, C. M. Cobley, and Y. N. Xia, Acc. Chem. Res. **41**, 1587 (2008).
8. D. H. Wang, D. Y. Kim, K. W. Choi, J. H. Seo, S. H. Im, J. H. Park, O. O. Park, and A. J. Heeger, Angew. Chem. Int. Ed. **50**, 5519 (2011).
9. S. W. Heo, E. J. Lee, K. W. Song, J. Y. Lee, and D. K. Moon, Org. Electron. **14**, 1931 (2013).
10. E. Giorgetti, A. Giusti, F. Giammanco, P. Marsili, and S. Laza, Molecules **14**, 3731 (2009).
11. D. Wang, M. Chen, X. Liu, and X. Gao, Chin. Opt. Lett. **13**, 081404 (2015).
12. S. Li, D. M. Wang, Z. Y. Wang, Z. W. Wang, M. Chen, and X. D. Liu, RSC. Adv. **5**, 63233 (2015).
13. S. Li, M. Chen, and X. D. Liu, Opt. Express **22**, 18707 (2014).
14. H. B. Zeng, X. W. Du, S. C. Singh, S. A. Kulinich, S. Yang, J. P. He, and W. P. Cai, Adv. Funct. Mater. **22**, 1333 (2012).
15. H. B. Zeng, W. P. Cai, Y. Li, J. L. Hu, and P. S. Liu, J. Phys. Chem. B **109**, 18260 (2005).
16. Z. J. Yan, R. Q. Bao, Y. Huang, A. N. Caruso, S. B. Qadri, C. Z. Dinu, and D. B. Chrisey, J. Phys. Chem. C **114**, 3869 (2010).
17. Z. J. Yan, R. Q. Bao, C. M. Busta, and D. B. Chrisey, Nanotechnology **22**, 265610 (2011).
18. Z. Y. Lin, J. L. Li, Z. Q. Zheng, J. H. Yan, P. Liu, C. X. Wang, and G. W. Yang, ACS Nano. **9**, 7256 (2015).